Slemr, F., Brenninkmeijer, C. A., Rauthe-Schöch, A., Weigelt, A., Ebinghaus, R., Brunke, E. G., Martin, L., Spain, T. G., & O'Doherty, S. (2016). El Niño-Southern Oscillation influence on tropospheric mercury concentrations. *Geophysical Research Letters*, *43*(4), 1766-1771. https://doi.org/10.1002/2016GL067949

AGU PUBLICATIONS

Geophysical Research Letters

RESEARCH LETTER
10.1002/2016GL067949

Key Points:
- Tropospheric Hg concentrations correlate with SOI with a lag of 6 to 12 months
- ENSO driven Hg variability is similar to CO which is driven by emissions from biomass burning (BB)
- The amplitude of Hg interannual variability is consistent with BB being the major driving force

Correspondence to:
F. Slemr,
franz.slemr@mpic.de

Citation:
Slemr, F., C. A. Brenninkmeijer, A. Rauthe-Schöch, A. Weigelt, R. Ebinghaus, E.-G. Brunke, L. Martin, T. G. Spain, and S. O'Doherty (2016), El Niño–Southern Oscillation influence on tropospheric mercury concentrations, *Geophys. Res. Lett.*, *43*, 1766–1771, doi:10.1002/2016GL067949.

Received 26 JAN 2016
Accepted 2 FEB 2016
Accepted article online 5 FEB 2016
Published online 25 FEB 2016

El Niño–Southern Oscillation influence on tropospheric mercury concentrations

Franz Slemr[1], Carl A. Brenninkmeijer[1], Armin Rauthe-Schöch[1], Andreas Weigelt[2,3], Ralf Ebinghaus[2], Ernst-Günther Brunke[4], Lynwill Martin[4], T. Gerard Spain[5], and Simon O'Doherty[6]

[1]Max Planck Institute for Chemistry, Mainz, Germany, [2]Helmholtz-Zentrum Geesthacht, Institute of Coastal Research, Geesthacht, Germany, [3]Now at Bundesamt für Seeschifffahrt und Hydrographie, Hamburg, Germany, [4]South African Weather Service c/o CSIR, Stellenbosch, South Africa, [5]School of Physics, National University of Ireland, Galway, Ireland, [6]School of Chemistry, University of Bristol, Bristol, UK

Abstract The El Niño–Southern Oscillation (ENSO) affects the tropospheric concentrations of many trace gases. Here we investigate the ENSO influence on mercury concentrations measured in the upper troposphere during Civil Aircraft for the Regular Investigation of the atmosphere Based on an Instrumented Container flights and at ground at Cape Point, South Africa, and Mace Head, Ireland. Mercury concentrations cross-correlate with Southern Oscillation Index (SOI) with a lag of 8 ± 2 months. Highest mercury concentrations are always found at the most negative SOI values, i.e., 8 months after El Niño, and the amplitude of the interannual variations fluctuates between ~5 and 18%. The time lag is similar to that of CO whose interannual variations are driven largely by emissions from biomass burning (BB). The amplitude of the interannual variability of tropospheric mercury concentrations is consistent with the estimated variations in mercury emissions from BB. We thus conclude that BB is a major factor driving the interannual variation of tropospheric mercury concentrations.

1. Introduction

The El Niño–Southern Oscillation (ENSO) affects tropical meteorological fields and has a large impact on atmospheric composition [*Inness et al.*, 2015, and references therein]. Its influence is exerted by changing the large-scale Walker circulation and associated convection and precipitation patterns. The changing precipitation patterns lead to draughts in Indonesia and many other regions of the world (El Niño events) which foster large-scale biomass burning not only in Indonesia [*Fuller and Murphy*, 2006] but also in Siberian and North American boreal forests [*Monks et al.*, 2012]. Because biomass burning is one of the major sources of atmospheric CO, CH_4, CH_3Cl, and many other trace gases and aerosols [*Andreae and Merlet*, 2001], the observed interannual variations of many of these gases could be shown to be driven by ENSO [e.g., *Wang et al.*, 2004; *Simmonds et al.*, 2005; *Logan et al.*, 2008; *Chandra et al.*, 2009; *Voulgarakis et al.*, 2010; *Inness et al.*, 2015].

Brunke et al. [2016] noticed that the annual average mercury concentrations in the atmosphere and in rainwater at Cape Point, South Africa, correlate with annual precipitation depth which in turn is also influenced by ENSO in southern Africa. This finding prompted us to analyze several atmospheric mercury data sets in detail, each of which encompasses more than 8 years of measurements. We use upper tropospheric data from monthly Civil Aircraft for the Regular Investigation of the atmosphere Based on an Instrumented Container (CARIBIC) flights made from 2005 until 2014 [*Slemr et al.*, 2016] and mercury concentrations measured at ground at Cape Point, South Africa, in 1995–2004 [*Slemr et al.*, 2008] and 2007–2014 [*Slemr et al.*, 2015] and at Mace Head, Ireland, in 1996–2013 [*Weigelt et al.*, 2015]. As will be discussed further below we find ENSO signatures in all these data sets.

2. Experimental

Since May 2005 mercury is being measured using a new CARIBIC measurement container on board a Lufthansa passenger Airbus 340-600 [*Brenninkmeijer et al.*, 2007; *Slemr et al.*, 2016]. Usually the container flies a monthly sequence of four consecutive intercontinental flights from Germany to airports in America, Asia, and Africa. The flight routes and the complete list of flights are given at www.caribic-atmospheric.com. In addition to a modified Tekran mercury analyzer (Tekran-Analyzer Model 2537 A, Tekran Inc., Toronto, Canada), the freight container holds automated analyzers for in situ measurements of CO, O_3, NO, NOy, CO_2, CH_4, total and gaseous water content, oxygenated organic compounds, and particles with diameter

larger than 4, 12, and 18 nm measured by three condensation nuclei counters and with diameter of 140–1050 nm measured by an optical particle size spectrometer. Moreover, air and aerosol samples are collected and subsequently analyzed in the laboratory for greenhouse gases, halocarbons, hydrocarbons, and particle elemental composition.

The air inlet system and the mercury instrument are described in detail by *Brenninkmeijer et al*. [2007] and *Slemr et al*. [2016]. We use a Tekran instrument, an automated dual channel, single amalgamation, cold vapor atomic fluorescence mercury analyzer. The instrument was modified for CARIBIC use essentially by inserting an additional PTFE diaphragm pump to keep the sampling flow rate at >0.5 L (standard temperature and pressure, STP, i.e., at 1013 hPa and 273.14 K) min^{-1} and an external computer to store the Tekran signal, ancillary data, and to communicate with the container master computer. The latter controls the operation of all instruments in the container and activates the pumps of the Hg instrument only at an ambient pressure below 500 hPa to protect the instrument and the sampling lines from contamination near to the airports. Consequently, no measurements below an altitude of about 5 km are available, and most of the data originate from cruising altitudes of 10–12 km, i.e., upper troposphere (UT) and lowermost stratosphere.

Since April 2014 we reintegrate the raw Tekran signal using a homemade program modeled on an integration of GC peaks to remove a low bias of mercury concentrations measured with small mercury loads and to improve the precision and the detection limit of the instrument [*Slemr et al*., 2016]. The bias in the original UT data until February 2014 was removed using a correction function derived from the original Tekran data and the reintegrated raw signal [*Slemr et al*., 2016]. This correction also removes the bias mismatch in the original data which originated from different sampling times (5–15 min) and thus varying loads used in the measurements since May 2005. Speciation experiments on board the CARIBIC container are discussed in detail by *Slemr et al*. [2016], and they suggest that the measurements represent total mercury (TM) concentrations in air. For this paper the data from May 2005 until November 2014 were analyzed.

The Cape Point (CP) site (34°21′S, 18°29′E) is operated as one of the Global Atmospheric Watch (GAW) baseline monitoring observatories of the World Meteorological Organization (WMO). The station is located on the southern tip of Cape Peninsula within the Cape Point National Park on top of a peak 230 m above sea level and about 60 km south from Cape Town. The station has been in operation since the end of the 1970s, and its current continuous measurements include those of Hg, CO, O_3, CH_4, N_2O, ^{222}Rn, CO_2, several halocarbons, particles, and meteorological parameters. The station receives clean marine air masses for most of the time. Gaseous elemental mercury (GEM) was measured by a manual amalgamation technique [*Slemr et al*., 2008] between September 1995 and December 2004 and by an automated Tekran 2537B instrument since March 2007 [*Slemr et al*., 2015]. Because of high humidity and sea salt coating of the sampling line and of an aerosol filter upstream of the instrument, we believe that sticky GOM (Gaseous Oxidized Mercury) will not get into the instrument and the measurements will thus primarily represent GEM (Gaseous Elemental Mercury). The Tekran instrument at CP has been run with a 15 min sampling frequency. Data until December 2014 are analyzed here.

The Mace Head (MH) GAW station is located on the western coast of Ireland at 53°20′N and 9°54′W. The nearest city is Galway at a distance of 55 km to the east. Galway has a population of about 75,000 and is the closest location of significant industrial activity. In addition to mercury, which is being measured since March 1996, a suite of meteorological parameters and other species is being monitored. These include O_3, CO, CO_2, CH_4, N_2O, and halocarbons, which aids the classification of incoming air masses. Atmospheric gaseous mercury is monitored by a Tekran analyzer. The instrument is operated with a temporal resolution of 15 min. With conditions similar to Cape Point we believe that only GEM is measured. Using meteorological analysis and a sophisticated Lagrangian dispersion model, the Mace Head data were attributed to four different air mass types: baseline, local, European polluted, and subtropical maritime [*Manning et al*., 2011]. Because local and European polluted air masses are per definition locally and regionally influenced, we analyze here only the baseline and subtropical maritime data until December 2013.

Only about half of the CARIBIC measurements originate from the troposphere. Stratospheric data were filtered out and rejected using potential vorticity (PV > 1 PVU) and ozone (O_3 > 80 ppb) criteria. Also, mercury concentrations higher than 2 ng m^{-3} were eliminated from the data set, because they are usually found only in plumes of polluted air [*Slemr et al*., 2014]. Monthly values of 3 month running medians and averages were calculated for the 0–30°N and 30–60°N latitude bands and tested for a meaningful trend. Because no secular trend was found in the monthly medians or in the averages for both latitudinal data sets, the data were directly correlated with a

Table 1. Cross Correlation of Monthly Values of Total Mercury (TM) (CARIBIC), Detrended (Relative) Gaseous Elemental Mercury (GEM) Concentrations (Cape Point, South Africa, and Mace Head, Ireland), and Deseasonalized (Relative) CO Mixing Ratios (All as Monthly Values of 3 Month Running Medians) With a 3 Month Running Average of SOI (www.cpc.Ncep.Noaa.gov/Data/Indices/soi.3m.txt)[a]

Site and Period	Equation	*R*, *n*, Significance	Hg Delay (Month)
CARIBIC 2007–2014, 0–30°N	TGM = −(0.0691 ± 0.0159) * SOI + (1.3990 ± 0.0167)	0.4223, 84, >99.9%	8 (8–10)
	COrel = −(0.0373 ± 0.0115) * SOI + (1.0115 ± 0.0109)	0.3429, 81, >99%	12 (11–13)
CARIBIC 2007–2014, 30–60°N	TGM = −(0.0652 ± 0.0162) * SOI + (1.5033 ± 0.0168)	0.3992, 87, >99.9%	6 (6–8)
	COrel: no significant correlation		
Cape Point 2007–2014	GEMrel = −(0.0457 ± 0.0063) * SOI + (1.0247 ± 0.0066)	0.6194, 86, >99.9%	10 (9–11)
	COrel = −(0.0367 ± 0.0052) * SOI + (1.0355 ± 0.0054)	0.6121, 86, >99.9%	10 (9–11)
Cape Point 1995–2004	GEMrel = −(0.0140 ± 0.0061) * SOI + (1.0032 ± 0.0050)	0.2404, 89, >95%	7 (6–8)
	COrel = −(0.0192 ± 0.0049) * SOI + (1.0024 ± 0.0041)	0.3621, 104, >99.9%	4 (4–6)
Mace Head "baseline" 1996–2013	GEMrel = −(0.0161 ± 0.0056) * SOI + (1.0029 ± 0.0053)	0.2062, 187, >99%	9 (8–10)
	COrel = −(0.0606 ± 0.0067) * SOI + (1.0188 ± 0.0062)	0.5408, 200, >99.9%	9 (8–10)
Mace Head "subtropical maritime" 1996–2013	GEMrel = −(0.0121 ± 0.0052) * SOI + (1.0022 ± 0.0050)	0.1727, 177, >95%	10 (10–11)
	COrel = −(0.0584 ± 0.0074) * SOI + (1.0192 ± 0.0070)	0.4932, 195, >99.9%	8 (7–9)

[a]The delay given in the last column is the one with the highest *R*. The delays in brackets are with the second and third highest significances of at least 95%.

3 month running average SOI (www.cpc.ncep.noaa.gov/data/indices/soi.3m.txt). We prefer 3 month SOI running averages, since the smoothed SOI corresponds better with other ENSO indices [*Fuller and Murphy*, 2006] and because it roughly matches the hemispheric mixing time of ~3 months [*Warneck*, 1987].

The GEM data sets from CP and MH display pronounced secular trends [*Slemr et al*., 2008, 2015; *Weigelt et al*., 2015] which tend to hide interannual variations [*Fuller and Murphy*, 2006]. We have thus detrended the monthly data (all as 3 month running medians) using trends obtained by the linear least square (LSQ) fit of the monthly medians. Mercury concentrations at CP show a downward trend in 1995–2004 and an upward one since 2007. Consequently, these two data sets were treated separately. Ratios of monthly medians to monthly concentrations calculated from their LSQ fit (relative GEM concentrations) are then used for the correlations with SOI. The correlations are repeated with ratios shifted month by month to earlier SOI values (cross correlation). Table 1 (last column) shows the lag which provided correlation with the highest *R*. As the *R* maximum is not very pronounced we give in brackets delays with the second and third highest *R* if significant. Monthly values of 3 month running median CO data were also cross-correlated with SOI. Detrending of the CO data was not necessary, because no significant trend was detected. However, the CO data were deseasonalized using the averages of monthly median CO mixing ratios over the measurement period.

All mercury concentrations are given in ng m^{-3} STP (i.e., at 1013 hPa and 273.14 K). We note that in correlations using 3 month running medians, the precision of individual Hg and CO measurements scales down with $\sqrt{n}$ to negligible values. Important is the internal consistency of each of the data sets. CO measurements at the GAW stations CP and MH were made in compliance with the WMO-GAW protocol [*World Meteorological Organization Global Atmospheric Watch*, 2010]. The continuous mercury measurements with the Tekran instruments at CP 2007–2014 and MH 1996–2013 were made in compliance with GMOS protocol (www.gmos.eu). The manual Hg technique used at CP in 1995–2004 is described in detail by *Slemr et al*. [2008]. The CO and Hg measurement techniques used on board CARIBIC are described by *Scharffe et al*. [2012] and *Slemr et al*. [2016], respectively. Bias mismatch due to varying sampling times in original Hg CARIBIC data set has been removed as mentioned before [*Slemr et al*., 2016].

3. Results and Discussion

Plots of the 3 month running medians and their correlations with the 3 month running SOI average are shown in Figure 1 for the CARIBIC data, and the statistical data including the CO correlations are listed in Table 1. Qualitatively, all Hg versus SOI and CO versus SOI plots are similar with the highest TM, relative GEM, and CO concentrations occurring at the most negative SOI values. Negative SOI values are related to El Niño events and positive SOI values to La Niña events. In addition, Table 1 shows that the TM or relative GEM concentrations always respond to SOI with a delay of 6–12 months. CO mixing ratios, with the exception of CARIBIC 30–60°N data, also cross-correlate with SOI with a delay of 4–13 months.

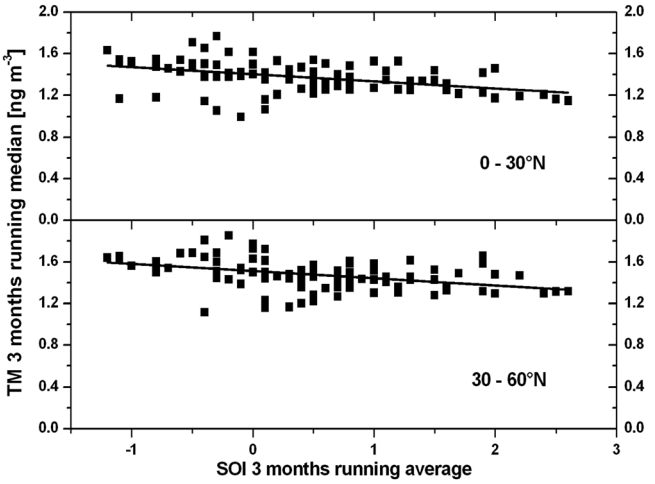

Figure 1. Correlation of 3 month running median tropospheric total mercury (TM) concentrations from CARIBIC measurements 2005–2014 with 3 month running average SOI. The slopes, intercepts, and lags against SOI, and the correlation significance are given in Table 1.

In quantitative terms, the correlations of CARIBIC monthly TM medians for 0–30°N and 30–60°N with SOI are very similar in slope and significance. The slightly higher intercept for the 30–60°N data is due to the North-South Hemispheric gradient. The correlations of CP relative monthly GEM medians in 2007–2014 and 1995–2004 differ both in slope and significance with a smaller slope and a lower significance in 1995–2004. The 2007–2014 data constitutes high-resolution Tekran data with an almost complete temporal coverage, whereas the monthly values of 3 month running medians in 1995–2004 are covered typically by only 150 h of measurements each (~50 individual measurements). This might be the reason for the lower significance of the 1995–2004 correlations. In addition, GEM monthly medians in 1995–2004 were decreasing [*Slemr et al.*, 2008] whereas in 2007–2014 they were increasing [*Slemr et al.*, 2015]. This may have some influence on the lag against SOI. The baseline and subtropical maritime MH data, on the other hand, correlate with the lowest significance of all. We tested whether this might be due to a changing baseline trend [*Weigelt et al.*, 2015] which is not taken into account by linear detrending over the whole 1996–2013 period. We found no influence, however. The somewhat lower significance for the southern maritime fraction in comparison with baseline air masses is most likely due to smaller data coverage: the baseline data representing 47.4% of all MH data, whereas the subtropical maritime component only amounted to 5.4% [*Weigelt et al.*, 2015]. We note that at CP and MH, the data from April 1997 to April 1998 and from August 1997 to May 1998, respectively, were missing. These missing data fall within the 1997 El Niño event, one of the most intensive and persistent El Niño events during the last 40 years [e.g., *Wang et al.*, 2004]. Even with these data gaps the CP 1995–2004 and MH data sets correlate with the SOI. CO data for CP 1995–2004 and MH covered the 1997 El Niño event, and this might be a reason for higher significance of their cross correlations with SOI in comparison with those of Hg. The significance of Hg versus SOI and CO versus SOI cross correlations is comparable for CP 2007–2014 data. The significance of CO versus SOI cross correlation for CARIBIC data from 0 to 30°N latitude band is smaller than for Hg versus SOI and insignificant for the 30–60° latitude band. This might be related to the fact that opposite to CP and MH the CARIBIC data are not baseline data. The spatial dimension in addition to the temporal one makes it almost impossible to filter out baseline data from the CARIBIC data set. The regional component will be larger for the shorter lived CO than longer lived Hg data. In addition, the 30–60° latitude band contains many flights to destinations such as Seoul, Beijing, Tokyo, and Osaka where pronounced urban/industrial plumes were observed.

The CARIBIC absolute slopes averaging at −0.067 have to be divided by the average mercury concentration of ~1.47 ng m^{-3} to convert it to relative slopes of −0.046 which agree well with the relative GEM slope of −0.046 for CP for the same period (Table 1). The relative GEM slopes for CP 1995–2004, MH baseline, and subtropical maritime data are with the range of −0.016 to −0.012 similar and substantially smaller than those for CARIBIC and CP 2007–2017 data. As already mentioned this might be due to missing data for the 1997 El Niño event in all these data sets. With exception of CP 1995–2004 data (and CARIBIC 30–60°N data with no significant correlation) the relative CO slopes vary from −0.037 for CARIBIC 0–30°N and CP 2007–2014 data to ~ −0.060 for both MH data sets and are within the same range as for the Hg versus SOI correlations.

The ranges of the lag of Hg and CO concentrations against SOI overlap for CP 2007–2014, 1995–2004, and MH baseline data sets and are close to those for CARIBIC 0–30°N and MH subtropical maritime data sets. The average lags of Hg versus SOI and CO versus SOI from the data in Table 1 are very similar with 8 ± 2 months for Hg and 7 ± 2 months for CO. The *R* maxima are rather broad for both Hg and CO correlations of all data sets. The delays of Hg and CO against SOI are, nevertheless, similar.

The ENSO influence on trace gas concentrations in both hemispheres can be induced by changing circulation patterns and/or driven by changes in emissions. Models and observations suggest that changes of ozone mixing ratios are due to a combination of dynamically induced and emission driven changes whereas the changes in CO mixing ratios are almost entirely driven by emissions from biomass burning [*Logan et al*., 2008; *Chandra et al*., 2009; *Voulgarakis et al*., 2010; *Inness et al*., 2015].

Dynamically induced changes are expected to react immediately to the changes in sea surface temperature and the circulation pattern related to them. An additional lag of 2–3 months might be needed to change the hemispheric mixing ratios. On the contrary, the lag of biomass burning against SOI is larger. Monthly fire counts in the Southeast Asia region lagged 4 months against the SOI [*Fuller and Murphy*, 2006]. *Skinner et al*. [2006] found that Canadian fires lagged 6 months against global sea surface temperature, i.e., against SOI. *Monks et al*. [2012] reported a 10–11 month lag of Arctic CO mixing ratios against the El Niño 3.4 index which is closely related to SOI [*Fuller and Murphy*, 2006]. The lag from these reports is similar to the lag of 7 ± 2 months found here. A lag of 8 ± 2 months of tropospheric Hg concentrations against SOI thus precludes the possibility of dynamically driven changes. Mercury evasion from the ocean surface is believed to be a major source of atmospheric mercury, accounting for some 45% of all emissions in the present-day atmospheric mercury cycle [*Selin et al*., 2008; *Holmes et al*., 2010; *Song et al*., 2015]. Since we would expect a rapid response of mercury evasion from sea surfaces to changes in sea surface temperature, the lagging tropospheric mercury concentrations also make oceanic emissions an unlikely source of the interannual mercury variability. The similar lags of tropospheric mercury concentration and CO mixing ratios suggest that the interannual variability of tropospheric mercury concentrations is predominantly driven by emissions from biomass burning.

With SOI spanning ~4 units the slopes translate to an amplitude of ~18% for the CARIBIC data from both latitude bands 0–30°N and 30–60°N; ~18% and ~6% for the Cape Point data in 2007–2014 and 1995–2004, respectively; and ~6% and ~5% for the Mace Head baseline and subtropical maritime data, respectively. The highest influence of the SOI on the CARIBIC data is probably related to the convection around the intertropical convergence zone (ITCZ) where a large proportion of the El Niño induced biomass burning occurs. The smaller relative amplitude at Cape Point 1995–2004 might be due to missing data from the El Niño 1997 event. The smaller relative amplitudes at Mace Head than at Cape Point 2007–2014 are probably caused by a smaller ratio of emissions from biomass burning relative to anthropogenic emissions in the Northern Hemisphere.

Annual CO emissions from biomass burning were estimated to vary between 169 and 565 Tg CO yr^{-1} during the 1996–2000 period [*Duncan et al*., 2003], between 337 and 591 Tg CO yr^{-1} during the 1997−2004 period [*van der Werf et al*., 2006], and between ~470 and 740 Tg CO yr^{-1} for the years 2006–2010 [*De Simone et al*., 2015]. *De Simone et al*. [2015] show that there are large differences between different biomass burning inventories. We note that the exceptionally strong 1997–1998 El Niño—with highest CO emissions—might be responsible for the larger interannual CO variability estimated by *Duncan et al*. [2003] and *van der Werf et al*. [2006]. Assuming Hg emissions from biomass burning to be proportional to those of CO, one would thus expect ~70% amplitude (relative to average) in Hg emissions from biomass burning. Estimates of mercury emissions from biomass burning relative to all mercury emissions vary between 3.6 and 9.0% [*Selin et al*., 2008; *Holmes et al*., 2010; *Pirrone et al*., 2010], respectively. Combined with the amplitude of CO emissions, this would imply an interannual variability of roughly 3–6% of all Hg emissions, if ENSO had an influence only on emissions from biomass burning. This is only about a quarter to half of the ENSO driven interannual amplitude of ~12% of tropospheric mercury concentrations derived here from SOI correlations. This difference suggests that the Hg emissions from biomass burning might be underestimated or that ENSO might influence other Hg emissions such as geogenic emissions, evapotranspiration, and volatilization [*Selin et al*., 2008; *Holmes et al*., 2010]. This conclusion, however, has to be considered as tentative because of the large uncertainties of estimated mercury emissions from biomass burning in general, its interannual variations (almost 100%) in particular [*De Simone et al*., 2015], and the uncertainty of our estimate.

4. Conclusions

We have investigated the ENSO influence on interannual variations of tropospheric mercury and CO concentrations measured in the upper troposphere during CARIBIC flights in 2007–2014 and at ground for Cape Point, South Africa, in 1995–2004 and 2007–2014 and at Mace Head, Ireland, in 1996–2014. We have found

an ENSO signature in all these data sets. Cross correlation of 3 month running median mercury concentrations 3with a 3 month running average SOI revealed that the tropospheric mercury concentrations lagged by 8 ± 2 months against the SOI while the amplitude of interannual mercury variations spanned ~5–18%. The highest mercury concentrations were always observed at most negative SOI values, i.e., on average 8 months after El Niño events. The lag of interannual variation of mercury concentrations against SOI is similar to the average lag of 7 ± 2 months for cross corelation of CO mixing ratios versus SOI. The interannual variations in CO mixing ratios are believed to be driven by emissions from biomass burning. We thus conclude that the variability of tropospheric mercury concentrations is primarily a function of biomass burning emissions. The observed amplitude of tropospheric mercury concentrations is, within large uncertainties, consistent with the variability estimated from the proportion of biomass burning emission to all mercury emissions.

Acknowledgments
We thank the CARIBIC, Cape Point, and Mace Head teams for the operation and maintenance of the Tekran instruments. Funding from the European Community within the GMOS (Global Mercury Observation System) project and from Fraport AG is thankfully acknowledged. The used data sets are available from the authors on request or from GMOS (www.gmos.eu), WMO-GAW (www.wmo.int), and CARIBIC (www.caribic-atmospheric.com) databases.

References

Andreae, M. O., and P. Merlet (2001), Emission of trace gases and aerosols from biomass burning, *Global Biogeochem. Cycles*, *15*, 955–966, doi:10.1029/2000GB001382.

Brenninkmeijer, C. A. M., et al. (2007), Civil aircraft for the regular investigation of the atmosphere based on an instrumented container: The new CARIBIC system, *Atmos. Chem. Phys.*, *7*, 1–24.

Brunke, E.-G., C. Walters, T. Mkololo, L. Martin, C. Labuschagne, B. Silvana, F. Slemr, A. Weigelt, R. Ebinghaus, and V. Sommerset (2016), Mercury in the atmosphere and rainwater at Cape Point, South Africa, *Atmos. Environ.*, *125*, 24–32.

Chandra, S., J. R. Ziemke, B. N. Duncan, T. L. Diehl, N. J. Livesey, and L. Froidevaux (2009), Effects of the 2006 El Niño on tropospheric ozone and carbon monoxide: Implications for dynamics and biomass burning, *Atmos. Chem. Phys.*, *9*, 4239–4249.

De Simone, F., S. Cinnirella, C. N. Gencarelli, X. Yang, I. M. Hedgecock, and N. Pirrone (2015), Model study of global mercury deposition from biomass burning, *Environ. Sci. Technol.*, *49*, 6712–6721.

Duncan, B. N., R. V. Martin, A. C. Staudt, R. Yevich, and J. A. Logan (2003) Interannual and seasonal variability of biomass burning emissions constrained by satellite observations, *J. Geophys. Res.*, *108*(D2), 4100, doi:10.1029/2002JD002378.

Fuller, D. O., and K. Murphy (2006), The ENSO–fire dynamics in insular Southeast Asia, *Clim. Change*, *74*, 435–455.

Holmes, C. D., D. J. Jacob, E. S. Corbitt, R. Mao, X. Yang, R. Talbot, and F. Slemr (2010), Global atmospheric model for mercury including oxidation by bromine atoms, *Atmos. Chem. Phys.*, *10*, 12,037–12,057.

Inness, A., A. Benedetti, J. Flemming, W. Huijnen, J. W. Kaiser, M. Parrington, and S. Remy (2015), The ENSO signal in atmospheric composition fields: Emission-driven versus dynamically induced changes, *Atmos. Chem. Phys.*, *15*, 9083–9097.

Logan, J. A., I. Megretskaia, R. Nassar, L. T. Murray, L. Zhang, K. W. Bowman, H. M. Worden, and M. Luo (2008), Effects of the 2006 El Niño on tropospheric composition as revealed by data from the Tropospheric Emission Spectrometer (TES), *Geophys. Res. Lett.*, *35*, L03816, doi:10.1029/2007GL031698.

Manning, A. J., S. O'Doherty, A. R. Jones, P. G. Simmonds, and R. G. Derwent (2011), Estimating UK methane and nitrous oxide emissions from 1990 to 2007 using an inversion modeling approach, *J. Geophys. Res.*, *116*, D02305, doi:10.1029/2010JD014763.

Monks, S. A., S. R. Arnold, and M. P. Chipperfield (2012), Evidence for El-Niño Southern Oscillation (ENSO) on Arctic CO interannual variability through biomass burning emissions, *Geophys. Res. Lett.*, *39*, L14804, doi:10.1029/2012GL052512.

Pirrone, N., et al. (2010), Global mercury emissions to the atmosphere from anthropogenic and natural sources, *Atmos. Chem. Phys.*, *10*, 5951–5964.

Scharffe, D., F. Slemr, C. A. M. Brenninkmeijer, and A. Zahn (2012), Carbon monoxide measurements onboard the CARIBIC passenger aircraft using UV resonance fluorescence, *Atmos. Meas. Tech.*, *5*, 1753–1760.

Selin, N. E., D. J. Jacob, R. M. Yantosca, S. Strode, L. Jaeglé, and E. M. Sunderland (2008), Global 3-D land-ocean-atmosphere model for mercury: Present-day versus preindustrial cycles and anthropogenic enrichment factors for deposition, *Global Biogeochem. Cycles*, *22*, GB2011, doi:10.1029/2007GB003040.

Simmonds, P. G., A. J. Manning, R. G. Derwent, P. Ciais, M. Ramonet, V. Kazan, and D. Ryall (2005), A burning question. Can recent growth rate anomalies in the greenhouse gases be attributed to large-scale biomass burning events?, *Atmos. Environ.*, *39*, 2513–2517.

Skinner, W. R., A. Shabbar, M. D. Flannigan, and K. Logan (2006), Large forest fires in Canada and the relationship to global sea surface temperatures, *J. Geophys. Res.*, *111*, D14106, doi:10.1029/2005JD006738.

Slemr, F., E.-G. Brunke, C. Labuschagne, and R. Ebinghaus (2008), Total gaseous mercury concentrations at the Cape Point GAW station and their seasonality, *Geophys. Res. Lett.*, *35*, L11807, doi:10.1029/2008GL033741.

Slemr, F., et al. (2014), Mercury plumes in the global upper troposphere observed during flights with the CARIBIC observatory from May 2005 until June 2013, *Atmosphere*, *5*, 342–369.

Slemr, F., et al. (2015), Comparison of mercury concentrations measured at several sites in the Southern Hemisphere, *Atmos. Chem. Phys.*, *15*, 3125–3133.

Slemr, F., et al. (2016), Atmospheric mercury measurements onboard the CARIBIC passenger aircraft, *Atmos. Meas. Tech. Discuss.*, doi:10.5194/amt-2015-376.

Song, S., et al. (2015), Top-down constraints on atmospheric mercury emissions and implications for global biogeochemical cycling, *Atmos. Chem. Phys.*, *15*, 7103–7125.

Van der Werf, G. R., J. T. Randerson, L. Giglio, G. J. Collatz, P. S. Kasibhatla, and A. F. Arellano Jr. (2006), Interannual variability in global biomass burning emissions from 1997 to 2004, *Atmos. Chem. Phys.*, *6*, 3423–3441.

Voulgarakis, A., N. H. Savage, O. Wild, P. Braesicke, P. J. Young, G. D. Carver, and J. A. Pyle (2010), Interannual variability of tropospheric composition: The influence of changes in emissions, meteorology and clouds, *Atmos. Chem. Phys.*, *10*, 2491–2506.

Wang, Y., R. D. Field, and O. Roswintiarti (2004), Trends in atmospheric haze induced by peat fires in Sumatra Island, Indonesia and El Nino phenomenon from 1973 to 2003, *Geophys. Res. Lett.*, *31*, L04103, doi:10.1029/2003GL018853.

Warneck, P. (1987), *Chemistry of the Natural Atmosphere*, pp. 24–26, Academic Press, San Diego, Calif.

Weigelt, A., R. Ebinghaus, A. J. Manning, R. G. Derwent, P. G. Simmonds, T. G. Spain, S. G. Jennings, and F. Slemr (2015), Analysis and interpretation of 18 years of mercury observations since 1996 at Mace Head, Ireland, *Atmos. Environ.*, *100*, 85–93.

World Meteorological Organization Global Atmospheric Watch (2010), Guidelines for the measurement of atmospheric carbon monoxide Report GAW No162, WMO Technical Document No. 1551, July 2010, Geneva, Switzerland.